PHYSICAL REVIEW C VOLUME 20, NUMBER 4 OCTOBER 1979

Proton optical model potential at sub-Coulomb energies for medium weight nuclei

S. Kailas*
Indiana University Cyclotron Facility, Bloomington, Indiana 47405

M. K. Mehta and S. K. Gupta
Nuclear Physics Division, Bhabha Atomic Research Centre, Bombay 400085, India

Y. P. Viyogi and N. K. Ganguly
Variable Energy Cyclotron Project, Bhabha Atomic Research Centre, Calcutta 700064, India
(Received 21 May 1979)

The (p,n) reaction excitation functions for eleven nuclei from $A = 45$ to 80 measured at proton energies below ~ 5 MeV have been analyzed utilizing the optical model. The real potential parameters used in the present work have been obtained by suitably combining the proton optical model parameters determined between 3 and 60 MeV. Large energy dependence of the real potential at energies below 5 MeV has been observed. The imaginary potential depths determined in the present analysis exhibit an anomalous behavior when plotted as a function of mass number A. By utilizing the low and intermediate energy proton data, an attempt has been made to obtain a "global" set of optical parameters in the proton energy range between 4 and 180 MeV, for medium weight nuclei.

[NUCLEAR REACTIONS ^{45}Sc, ^{48}Ca, ^{51}V, ^{54}Cr, ^{55}Mn, ^{59}Co, ^{61}Ni, ^{65}Cu, ^{71}Ga, ^{75}As, ^{80}Se; E below ~ 5 MeV, analyzed $\sigma_{p,n}$, optical model parameters.]

I. INTRODUCTION

The optical model has played a very useful role in systematizing a large amount of experimental data covering various target nuclides and a large range of projectile energies. There have been various attempts in literature[1] to determine a set of nucleon-nucleus optical model parameters for a large number of nuclides—"the global parameters." For protons, by analyzing the proton-nucleus scattering, reaction and polarization data, global optical model parameters have been determined covering the energy range ~10 to 60 MeV (Refs. 2–4) with reasonable success. However, there has been very little work[5] extending this type of analysis to lower proton energies. This becomes all the more interesting in view of the recent interesting findings of Johnson *et al.*[6] in their optical model analysis of (p,n) data for A ~90–130 at sub Coulomb energies. In the present work we give the results of optical model analysis covering several medium weight targets ($A = 45$–80) and for proton energies from ~2 to 5 MeV. In doing so, care has been taken to maintain consistency with the high energy data in extrapolation of relevant parameters to lower energies. The conventional method of finding optical model parameters through elastic scattering differential cross section measurement is not suitable at these low proton energies, as the elastic scattering at forward angles will be dominated by the Coulomb scattering, and at backward angles the contribution from compound elastic scattering may be comparable to the potential scattering. This being the case, the analysis has been performed in the present work by utilizing the $\sigma_{p,n}$ cross sections with the assumption $\sigma_{p,n} \approx$ total reaction cross section. This is a valid approach[6] to a large extent, as the (p,n) channel is the dominant reaction channel at these proton energies. The analysis has yielded global optical model parameters for the proton energies below ~5 MeV.

II. ANALYSIS

A. General background

The usual procedure followed by optical model analysts is to fit the scattering/reaction data of a target measured for a given projectile energy (energies) by varying the optical parameters suitably. This type of analysis extended to cover a large number of nuclides and performed for a range of projectile energies—the so-called global analysis—will yield meaningful parameters and systematics only if a few relevant parameters are varied to fit the data. For protons, Becchetti and Greenlees[3] have determined the global optical parameters by their systematic analysis of elastic differential cross sections and polarization data for $A > 40$ and for $E < 50$ MeV. Their parameters appear to give fairly good fits down to 10 MeV. Menet[4] *et al.*, utilizing the reaction data, extended this type of analysis to cover the proton energy range 30 to 60 MeV. Perey[2] has given an-

other set of parameters used exclusively at lower energies (~10 to 20 MeV) for medium weight nuclei $30 < A < 100$. However, there is very little work for lower proton energies. In an attempt to extend the optical model analysis to these low proton energies, we fitted the total (p,n) cross section data on a large number of nuclides (most of these measured at the Van de Graaff laboratory, Bombay, India) and determined parameters of interest in the proton energy range ~2 to 5 MeV, with the assumption $\sigma_{p,n} \sim \sigma_R$. For this analysis we made use of the (p,n) cross section data for the nuclides ^{48}Ca, ^{45}Sc, ^{51}V, ^{54}Cr, ^{55}Mn, ^{59}Co, ^{80}Se (our measurement[7]) and ^{61}Ni, ^{65}Cu, Ga, and ^{75}As [Data from ORNL-2910 (Ref. 8)] measured up to ~5 MeV proton energy. All the data are either with thick targets or with thin targets suitably averaged to smooth over the compound nucleus fine structures. As $\sigma_{p,n}$ ($\approx\sigma_R$) is expected to be the most sensitive to the imaginary potential, it was decided to fix up the real potential parameters and vary only the imaginary potential parameters to fit the data. By restricting the number of parameters to be varied, it was hoped some useful systematic behavior would emerge from the analysis. The computer code OMGLOB,[9] which has a provision to search for parameters to fit the data for a large number of nuclides and range of energies simultaneously, has been used throughout the analysis. An absolute experimental error of ~15% (20% for ^{48}Ca) has been used for all the data points. It should be pointed out that Johnson's group from Oak Ridge has also contributed significantly in this type of (p,n) reaction measurements and analysis[6,8,10,11] and the approach we follow here is similar to theirs in many respects.

The optical model used was a conventional sum of Woods-Saxon real potential and derivative Woods-Saxon imaginary potential and the Coulomb potential. The spin-orbit potential was not included as the reaction data were expected to be insensitive to this component of the potential. The optical potential employed is given by

$$V(r) = -V_R f(r, R_R, a_R) + i4a_D W_D \frac{d}{dr} f(r, R_D, a_D) + V_C(R_C), \quad (1)$$

where

$$f(r, R_x a_x) = \{1 + \exp[(r - R)/a_x]\}^{-1},$$

$$R = R_x A^{1/3},$$

$$V_R(E) = V_R(0) - V_{ER} E,$$

$V_C(R_C)$ = potential for a uniformly charged sphere,

$$V_R(0) = V_0 + V_{\text{sym}} \frac{N-Z}{A} + 0.4 \frac{Z}{A^{1/3}}.$$

B. Real potential parameters

Energy coefficient V_{ER}. To start with, the energy coefficient V_{ER} was fixed for these low proton energies by extrapolation of V_{ER} values determined at higher energies. In Fig. 1, the V_{ER} values found for the E ranges 30–60 MeV,[4] 10–50 MeV,[3] 9–22 MeV,[2] and 3–5 MeV (Ref. 10) are plotted (semilog paper) at the respective mean proton energies. The points seem to lie on a straight line and could be very well fitted by a function of the form $V_{ER} = 0.963 \exp(-0.0343E)$ (E is in MeV). Using this expression an average value of ~0.85 has been obtained for the proton energy range considered in the present work (average $E \sim 4$ MeV). This value of V_{ER} has been used throughout the analysis. This large increase of V_{ER} at these sub-Coulomb energies is not unexpected.[10,12] Eck and Thompson,[12] in their analysis of Pb and Bi proton scattering data at sub-Coulomb energies, find a value of $V_{ER} \gtrsim 1$. In Sec. III, we further discuss the behavior of V_{ER}.

Real potential depth, $V_R(0)$. As V_{sym} is not sensitive to energy variation (its values are 27, 24, 26.4) (Refs. 2–4), it was decided to keep it fixed at 24 MeV as given in Ref. 3. The geometry parameters R_R and a_R were also fixed at the values given in Ref. 3 to avoid variation of too many

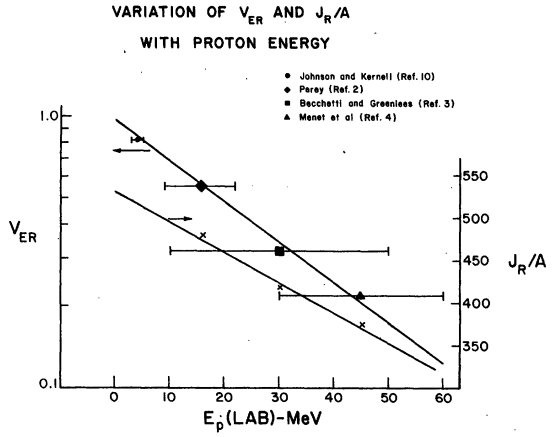

FIG. 1(a) Variation of real potential energy coefficient V_{ER} with proton energy, E. ●: Johnson and Kernell (Ref. 10); ♦: Perey (Ref. 2); ■: Becchetti and Greenlees (Ref. 3); ▲: Menet *et al.* (Ref. 4). The line is from the least square fit. (b) Variation of volume integral (J_R/A) with E. The points are from Refs. 2–4 for ^{59}Co. The line is from the least square fit.

parameters. Having fixed V_{BR}, V_{sym}, R_R, a_R, the parameter V_0 was determined as follows: Taking a nucleus say, ^{59}Co which fell in the global range of nuclides used in Refs. 2–4, the volume integral per nucleon was determined for the various proton energy ranges and using the respective optical model parameters. These volume integrals plotted as a function of E_p (corresponding to mean proton energies for the various ranges) exhibited a straight line behavior (Fig. 1). The least square fitted straight line extended to lower proton energies gave the volume integrals at the energies of interest to us (average $E \sim 4$ MeV). Using this volume integral and the parameters $V_{sym} = 24$, $R_R = 1.17$, $a_R = 0.75$, $V_{BR} = 0.85$, the central depth V_R was determined from the expression for volume integral

$$J_R = \tfrac{4}{3}\pi R^3 V_R \left(1 + \frac{\pi^2 a_R^2}{R^2}\right). \quad (2)$$

This gave a value of $V_0 \approx 59.2$. It should be mentioned that ^{59}Co is only a representative of the various nuclides considered in the global analysis and as such, one could get similar V_0 values starting from any other nucleus from the global set.

C. Imaginary potential parameters

Having determined the real potential parameters as mentioned above, we proceeded to find out the sensitive imaginary potential parameters. Again to limit the number of parameters searched to the minimum, the geometry parameters R_D and a_D were kept fixed at 1.32 and 0.58, respectively. The (p,n) reaction excitation function for each of the nuclides mentioned above was fitted (using the program OMGLOB[9]) by searching for best values of W_D. The W_D values determined for the various nuclides are plotted as a function of A (Fig. 2). The fits to (p,n) data are shown in Figs. 3 and 4. The fits in general are good. The X^2 (per point) values for the various cases were found to be less than 4. However, they were higher for Ga and As (~14 for Ga, ~10 for As). We believe that the W_D values determined in the present work would have a variation of ±20% around the mean values quoted in the present work. In order to see the sensitivity of W_D on a_D, the form of a_D of Ref. 3 [$0.51 + 0.7(N-Z)/A$] was also tried and W_D was found to be affected a little in magnitude, but the basic features with respect to variation with A remained unaltered. As the proton energy range scanned was small, it was decided not to introduce the

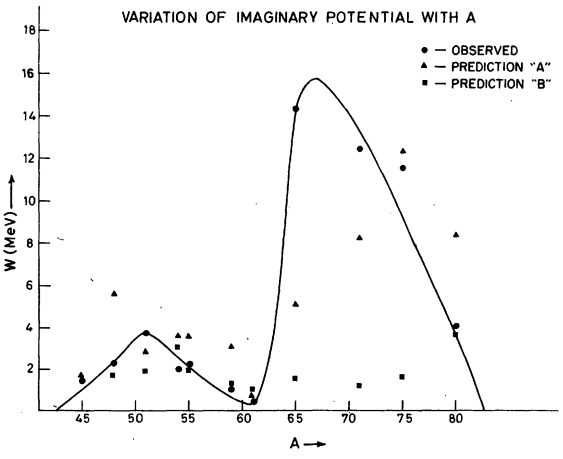

FIG. 2. The imaginary potential depth W_D as a function of A. The continuous line is drawn visually. The dots correspond to the values determined in the present work. Prediction A is based on number of open neutron channels; prediction B is based on deformation of target nuclei.

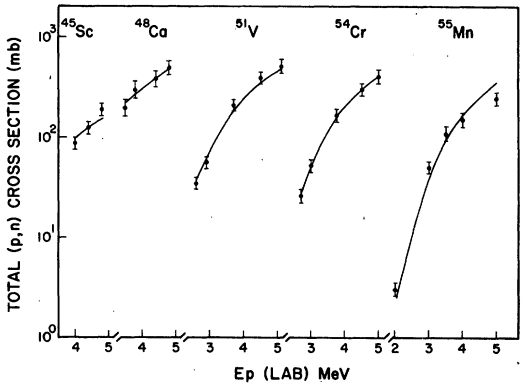

FIG. 3. Excitation functions for ^{45}Sc, ^{48}Ca, ^{51}V, ^{54}Cr, and ^{55}Mn and the optical model fits.

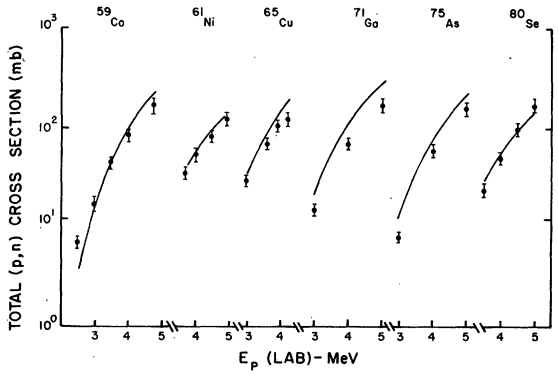

FIG. 4. Excitation function for ^{59}Co, ^{61}Ni, ^{65}Cu, ^{71}Ga, ^{75}As, and ^{80}Se and the optical model fits.

energy variation for W_D.

The interesting feature to be noted is the anomalous variation of W_D as a function of A (Fig. 2). (The curve drawn is just to guide the eye.) Johnson *et al.*[6] have also observed a similar behavior in their analysis of (p,n) data for $89<A<130$ at sub-Coulomb proton energies. It is interesting to explore why W_D does not have monotonic dependence on N, Z, and A, unlike other potential parameters. This point is further discussed in Sec. III.

D. Strength function analysis

In order to show the goodness of the fitting procedure followed here as well as to bring out any possible nuclear size effects, strength functions (for an average energy of 4 MeV) have been calculated for all the cases. The procedure followed in the present work is the same as that described in Refs. 10 and 11. The proton strength function (SFN) at energy E_p is defined as

$$S_p = S_{p,n} = \frac{\sigma_{pn}}{4\pi^2 k^{-2} \sum (2l+1) P_l} ,$$

where P_l is the Coulomb penetration factor for protons calculated at $R = 1.45A^{1/3}$ fm. The average SFN's for the various nuclei obtained from their respective excitation functions are plotted in Fig. 5 as a function of A. The error bars in Fig. 5 correspond to the variation of SFN over the energy range over which the excitation function has been measured. As can be seen from the figure, the agreement of experimental SFN with the corresponding theoretical estimate (obtained from optical model fits) is good for most of the cases. However, there is a marked deviation for Ga and As cases. This is because of the poor fits for $\sigma_{p,n}$ obtained for these nuclei. The above plot goes through a maximum for $A \simeq 51$. This might correspond to the D wave size resonance predicted a long time ago by Schiffer *et al.*[13] According to them, the S wave resonance is expected to be around $A \sim 68$. We do not have enough data in this mass region to bring out this fact, but there is an indication for a rise in SFN for ^{65}Cu and a depression in SFN for ^{71}Ga. The observed variation of SFN with A is similar to that seen for W and this brings out the close connection between SFN and W.

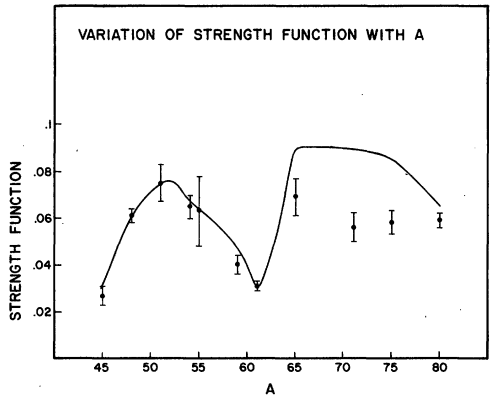

FIG. 5. Variation of proton strength function with A.

III. DISCUSSION

A. Real potential

The energy coefficient V_{ER} found in the present work is +0.85 and indicates that $|V_{ER}|$ increases with a decrease of proton energy. To understand this behavior much better we have carried out an analysis similar to the one performed by Eck and Thompson.[12] Following Ref. 12 we define $\gamma_R = -V_{ER}/V_R$. The γ_R values for the various proton energy ranges considered above have been determined from literature quoted V_{ER} and V_0 values.[2,3,4] These γ_R values along with the one found in the present work are plotted in Fig. 6(a) as a function of E. We have also calculated the nonlocality parameter d following the approach of Ref. 12. Using the expressions[12]

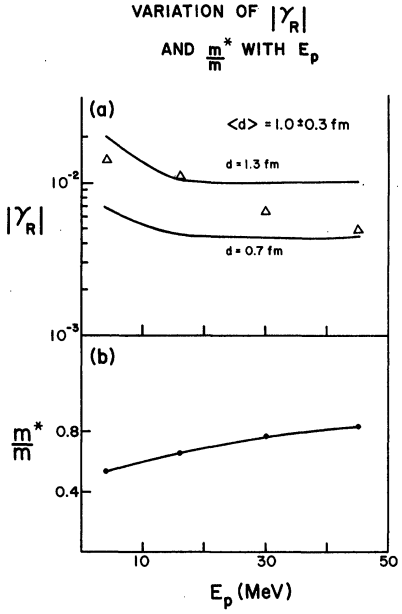

FIG. 6(a). The plot of $|\gamma_R|$ with E ($|\gamma_R| = V_{ER}/V_R$). (b) The ratio of the effective mass m^* and the nucleon mass m plotted as a function of E. The continuous line is drawn to guide the eye.

$$E=\frac{Ze^2}{r_T}-\frac{V_R}{1+\exp[(r_T-R)/a_R]} \tag{4a}$$

and

$$\gamma_R=\frac{-1}{\dfrac{V_R}{1+\exp\dfrac{(r_T-R)}{a_R}}+\dfrac{2\hbar^2}{md^2}}, \quad E\sim B_c \tag{4b}$$

and

$$\gamma_R=\frac{-1}{V_R+2\hbar^2/md^2}, \quad |E-B_C|\gg 0 \tag{5}$$

(in the above expressions, B_C is the Coulomb barrier height) and the γ_R values determined for the various proton energy ranges mentioned above, we have obtained an average value of 1 ± 0.3 for the nonlocality parameter d. In Fig. 6(a) we have shown the γ_R values calculated using expressions (4) and (5) for $d=0.7$ and 1.3 fm. It was found that γ_R extracted from phenomenological analyses lie between these predictions. The value of $d=1\pm0.3$ obtained from the present analysis is in good agreement with the standard values[12] 0.85 or 1.39 fm, normally quoted for d. This analysis shows that the large variation of V_{ER} with E at low energies is a consequence of using a local potential to approximate a nonlocal potential and not in disagreement with the values determined at higher energies.

We define, following Ref. 12, the ratio of the effective mass m^* and the nucleon mass as $m^*/m = 1/(1+V_{ER})$. We have computed m^*/m for the various V_{ER}, E combinations discussed above, and plotted in Fig. 6(b) the variation of m^*/m with E. It was found that m^*/m changes by 40–50% in going from 4 to 50 MeV. This behavior was similar to what had been observed in Ref. 12.

B. Imaginary potential

As pointed out earlier, the variation of W with A has come out to be anomalous. Earlier Johnson *et al.*[6] had also found a similar behavior of W with A in their analysis of (p,n) data for $89\lesssim A\lesssim 130$. If we combine their findings with that of ours, we find that W goes through maxima for A values ~52, 67, and 103, and minima for $A\sim 42$, 61, 84, and 120. A plot of $A^{1/3}$ ($=R$) versus maxima (minima) number, Fig. 7, appears to follow a straight line and this indicates the presence of some systematics perhaps related to some size effects. The minima around $A\sim 42$, 61, 84, and 120 could be due to proton shell (subshell) closures for $Z=20$, 28, 40, and 50. The present conclusions are tentative.

We have also observed some interesting correlations between the W values determined for the various A_Z^N and the level densities of the corresponding residual nuclei, A_{Z+1}^{N-1} (the number of open neutron channels[14] for $E_p\sim 4$ MeV). By normalizing the level density sum for all the A considered here with that of the W sum, we have determined equivalent W values for the various nuclei from their respective level densities. These predictions (prediction A) are plotted in Fig. 2 and there appears to be a good correspondence between the W values and level densities.

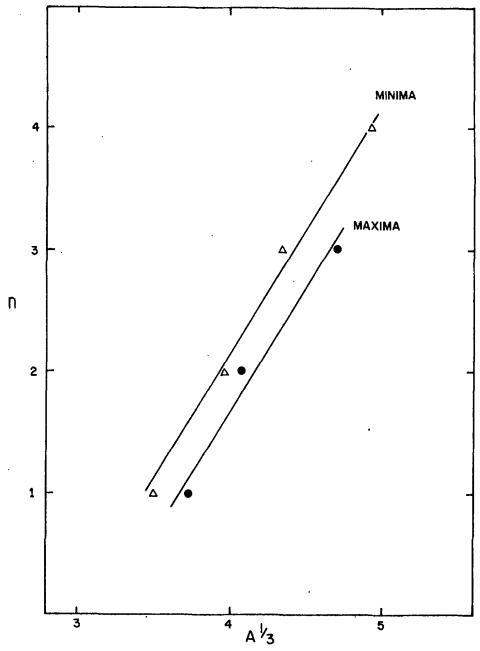

FIG. 7. The positions (or the number) of maxima (minima) of W as a function of $A^{1/3}$ ($=R$). The straight lines are drawn for visual guidance.

In analyzing deuteron scattering data, Hjorth *et al.*[15] have obtained the following linear relation connecting J_I/A and $[B(E20^+\rightarrow 2^+)]^{1/2}/A$ for the various nuclei: $J_I/A=x+y[B(E2)]^{1/2}/A$, x and y are constants. This is an interesting result as it shows the absorption per unit size (J_I/A) is proportional to the softness of the core $[B(E2)/A]$ and hence brings the connection between the imaginary potential and nuclear structure of target nucleus. Following Ref. 15 we plotted the $B(E2)/A$ vs J_I/A curve by considering the nuclides in the present work. The $B(E2)$ values were obtained by considering the transition between the first excited state and the ground state from Ref. 14. We found that but for Cu, Ga, and As—the anomalously behaving nuclides—the above mentioned linear relationship between $B(E2)/A$ and J_I/A was good for the nuclides considered here. We have also calculated the W values for the various cases starting from this linear relation and plotted these predictions (prediction B) in Fig. 2. Once again we find

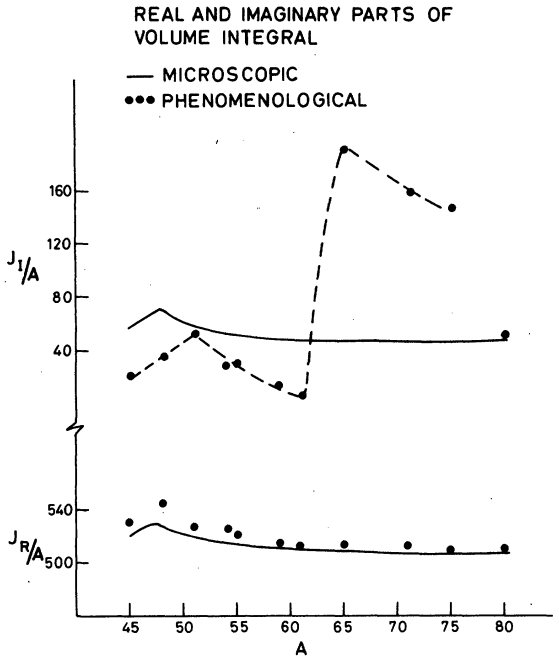

FIG. 8. Volume integrals for the real and imaginary parts of the optical potential obtained from phenomenological analysis compared with the microscopic predictions. The dashed line is drawn visually.

that the predicted W values (except for Cu, Ga, and As) are in good accord with the values obtained from phenomenological analysis.

We have tried to explain the observed behavior of W with A in terms of shell effects, neutron level densities, and deformation effects, with limited success. Though the overall variation of W with A is explainable in terms of the above mentioned quantities, the anomalous behavior of W with A is still not fully understood.

C. Comparison with microscopic approach

As a further check on the potentials determined in the present work, the volume integrals for both the real and imaginary potentials have been calculated and compared with the same quantities computed from the microscopic optical model potentials of Jeukenne *et al.*[16] In Fig. 8 we have plotted the volume integrals as a function of A. It is found that the volume integrals for the real potential agreed within 1–3% with that of microscopic predictions. However, imaginary potentials deviate considerably from that of the microscopic calculation. As in Fig. 2, they exhibit a resonance-like behavior when plotted as a function of A (the dashes in Fig. 8 are just to guide the eye).

D. Global optical parameters

Recently, Nadasen *et al.*[17] have obtained proton optical model parameters in the E_p range between 80 and 180 MeV by analyzing the scattering data on Si, Ca, Zr, and Pb targets. We have made an attempt to combine the present work with that of Ref. 17 to generate global optical model parameters for the E_p range between 4 and 180 MeV. In Fig. 9 we have plotted the typical J_R/A and J_I/A

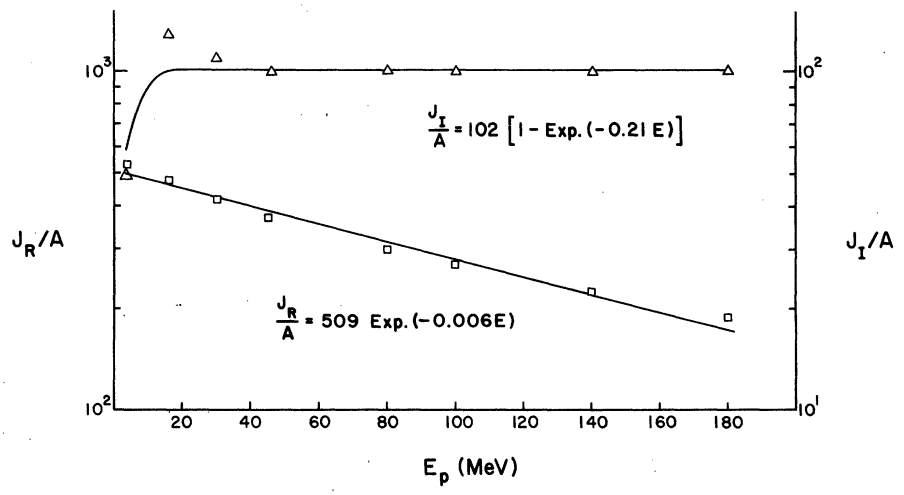

FIG. 9. Energy dependence of the volume integrals for the real and imaginary potentials.

values obtained from the present work, Refs. 2, 3, 4, and 17 and fitted them with the expressions

$$\frac{J_R}{A} = 509 \exp(-0.006E)$$

and

$$\frac{J_I}{A} = 102[1 - \exp(-0.21E)].$$

The observed variation of J_R/A and J_I/A with E_p is in good agreement with the theoretical calculations of Ref. 18. From the above analysis, we propose the following set of optical model parameters in the proton energy range between 4 and 180 MeV, for medium weight nuclei ($40 > A < 80$):

$$\frac{J_R}{A} = 509 \exp(-0.006E) \text{ MeV fm}^3,$$

$$R_R = 1.17, \quad a_R = 0.75, \quad V_{\text{sym}} = 24 \text{ MeV},$$

$$\frac{J_I}{A} = 102[1 - \exp(-0.21E)] \text{ MeV fm}^3,$$

$$R_D = 1.32, \quad a_D = 0.58.$$

IV. CONCLUSION

The proton optical model parameters at energies below 5 MeV have been obtained by analyzing the (p,n) cross section data on a large number of nuclides between $A = 45$ and 80. These parameters, besides their inherent interest in revealing the general behavior of optical model at these low energies, are expected to play a useful role in the microscopic determination of nucleus-nucleus potentials where one requires as input nucleon-nucleus potentials from a very low to high energies. The interesting feature of the present work is the curious behavior of W with A. The present data combined with that of Ref. 6 seem to indicate the presence of a size effect as a possible cause for the anomalous behavior of W. Interesting correlations have been obtained between the W values, the number of open neutron channels of residual nuclei, and deformation of target nuclei. It is encouraging that energy dependent expressions for J_R/A and J_I/A can be obtained in the E_p range between 4 and 180 MeV, which fit well the phenomenological estimates.

*Permanent address: Nuclear Physics Division, Bhabha Atomic Research Centre, Bombay 400085 India.

[1]C. M. Perey and F. G. Perey, At. Data Nucl. Data Tables 17, 1 (1976).
[2]F. G. Perey, Phys. Rev. 131, 745 (1963).
[3]F. D. Becchetti, Jr. and G. W. Greenlees, Phys. Rev. 182, 1190 (1969).
[4]J. J. H. Menet, E. E. Gross, J. J. Malanify, and A. Zucker, Phys. Rev. C 4, 1114 (1971).
[5]S. Kailas, S. K. Gupta, M. K. Mehta, S. S. Kerekatte, L. V. Namjoshi, N. K. Ganguly, and S. Chintalapudi, Phys. Rev. C 12, 1789 (1975).
[6]C. H. Johnson, A. Galonsky, and R. L. Kernell, Phys. Rev. Lett. 39, 1604 (1978).
[7,8] ^{48}Ca: Gulzar Singh, S. Saini, S. Kailas, A. Chatterjee, M. Balakrishnan, and M. K. Mehta, Nucl. Phys. Solid State Phys. (India) 19B, 29 (1976); ^{45}Sc: K. V. K. Iyengar, S. K. Gupta, K. K. Sekharan, M. K. Mehta, and A. S. Divatia, Nucl. Phys. A96, 521 (1967); ^{51}V: M. K. Mehta, S. Kailas, and K. K. Sekharan, Pramāna 9, 419 (1977); ^{54}Cr, ^{59}Co: Ref. 5; ^{55}Mn: Y. P. Viyogi, P. Satyamurthy, N. K. Ganguly, S. Kailas, S. Saini, and M. K. Mehta, Phys. Rev. C 18, 1178 (1978); ^{80}Se: S. Kailas, N. K. Ganguly, M. K. Mehta, S. Saini, N. Veerabahu, and Y. P. Viyogi, Nucl. Phys. A315, 157 (1979).
[8] ^{61}Ni, ^{65}Cu, Ga, and ^{75}As: C. H. Johnson, A. Galonsky, and C. N. Inskeep, Report No. ORNL-2910, 1960 (unpublished), pp. 25–28.
[9]Y. P. Viyogi and N. K. Ganguly, Bhabha Atomic Research Centre (BARC) report (unpublished).
[10]C. H. Johnson and R. L. Kernell, Phys. Rev. C 2, 639 (1970).
[11]C. H. Johnson, J. K. Bair, C. M. Jones, S. K. Penny, and D. W. Smith, Phys. Rev. C 15, 196 (1977).
[12]J. S. Eck and W. J. Thompson, Nucl. Phys. A237, 83 (1975).
[13]J. P. Schiffer and L. L. Lee, Jr., Phys. Rev. 109, 2098 (1958).
[14]Nucl. Data Sheet, B 3–5, 6–37 (1970); B 3–5, 6–161 (1970); B 4, 237 (1970); B 4, 351 (1970); 10, 205 (1973); 15, 289 (1975); 16, 1 (1975); 16, 25 (1975); 16, 351 (1975); 17, 485 (1976); 18, 463 (1976).
[15]S. A. Hjorth, E. K. Lin, and A. Johnson, Nucl. Phys. A116, 1 (1968).
[16]J. P. Jeukenne, A. Lejeune, and C. Mahaux, Phys. Rev. C 16, 80 (1977).
[17]A. Nadasen, P. Schwandt, P. P. Singh, A. D. Bacher, P. T. Debevec, W. W. Jacobs, M. D. Kaitchuck, and J. T. Meek (unpublished).
[18]G. Passatore, Nucl. Phys. A95, 694 (1967); A110, 91 (1968).